Processing and Application of Ceramics 13 [4] (2019) 349–359
https://doi.org/10.2298/PAC1904349Q

A comparative study on the dielectric and multiferroic properties of $Co_{0.5}Zn_{0.5}Fe_2O_4/Ba_{0.8}Sr_{0.2}TiO_3$ composite ceramics

Xiaofeng Qin[1,2], Ruicheng Xu[1,2], Heng Wu[1,2], Rongli Gao[1,2,*], Zhenhua Wang[1,2], Gang Chen[1,2], Chunlin Fu[1,2], Xiaoling Deng[1,2], Wei Cai[1,2,*]

[1]*School of Metallurgy and Materials Engineering, Chongqing University of Science and Technology, Chongqing 401331, China*
[2]*Chongqing Key Laboratory of Nano/Micro Composite Materials and Devices, Chongqing 401331, China*

Received 19 January 2019; Received in revised form 7 August 2019; Accepted 4 October 2019

Abstract

$Co_{0.5}Zn_{0.5}Fe_2O_4/Ba_{0.8}Sr_{0.2}TiO_3$ (CZFO/BST) composite ceramics with different molar ratios (1:3, 1:2, 1:1, 2:1 and 3:1) were prepared by combining chemical co-precipitation and sol-gel method. Effects of molar ratio on the microstructure, dielectric and multiferroic properties were investigated. The formation of the individual phases and the composites was confirmed by XRD results and small amount of secondary phase ($Ba_2Fe_2Ti_4O_{13}$) was observed. The grain sizes of magnetic (CZFO) and ferroelectric phase (BST), measured by SEM, were about 5 μm and 0.5 μm, respectively. The sample with molar ratio (1:2) has the largest dielectric constant, while the sample with molar ratio (3:1) shows the lowest dielectric constant. A distinct loss peak can be observed for all the samples. Both the peak position and peak intensity increase with the frequency, indicating relaxation polarization process generated by space charge or interface polarization. The ceramics with molar ratio (1:1) shows the smallest leakage current (~ 10^{-7} A/cm at 1.5 kV/cm), while the leakage current (~ 10^{-5} A/cm at 1.5 kV/cm) of the sample with molar ratio (3:1) is the largest. The ferroelectric hysteresis loop is not apparent due to the low Curie temperature of the ferroelectric phase, but the sample with molar ratio (2:1) shows the best ferroelectric properties. It was found that with the increase of CZFO content, the values of saturation (M_s) and remnant (M_r) magnetization increase at first and then decrease. The sample with molar ratio (3:1) has the maximum M_s value (about 50.34 emu/g), while the sample with molar ratio (1:2) shows the minimal M_r value (about 0.46 emu/g). This anomalous magnetic property is induced by the interface interaction between the two phases.

Keywords: *CZFO/BST, composite ceramics, dielectric, ferroelectric and magnetic properties*

I. Introduction

Multiferroic materials, which show magnetic and ferroelectric properties simultaneously, have attracted great attention for many years due to their intriguing physical properties and potential applications in modern society [1–3]. Particularly, in these materials the magnetic properties can be tuned under the action of external electric filed, and the ferroelectric properties are also affected by the applied magnetic field. This phenomenon is called magnetoelectric (ME) coupling effect. As a result, these materials have fascinated many researchers for their ability to perform different functions simultaneously. They are promising candidates for potential use in many new-type and multi-functional devices, such as spintronic devices, transducer, storage, capacitor etc. [4–6]. In recent years, in order to develop materials with new multi-functionality, multiferroics exerts a tremendous fascination of researchers. Although the ME coupling effect has been reported in single phase materials for many years, it is usually very weak at room temperature, limiting their practical applications. In general, this weak ME effect is result of the low Curie temperature (T_C) of the single phase multiferroic materials. The Curie temperatures of most single phase multiferroic materials are far below room temperature, thus the

*Corresponding author: tel: +7 4822 581493,
e-mail: *gaorongli2008@163.com* (Rongli Gao),
caiwei_cqu@163.com (Wei Cai)

ME effect can be observed only at low temperature.

As an exceptional case, $BiFeO_3$ (BFO) is a typical single phase multiferroic material with high Curie temperature ($T_C \sim 1100$ K) and Neel temperature ($T_N \sim 640$ K) [7–9]. In addition, the remnant polarization ($P_r \sim 100\,\mu C/cm^2$) of BFO is high and the band gap ($E_g \sim 2.7$ eV) is lower than that for many other ferroelectric materials causing that BFO attracted extensive attention worldwide because of its excellent properties and therefore potential applications [10,11]. However, the ME effect in BFO is very weak mostly due to the leakage current and weak magnetization at room temperature [12–14]. On one hand, impurities are prone to be formed due to the volatilization of Bi element at high temperature in the sintering process. On the other hand, defects such as oxygen vacancies are usually generated in these perovskite oxides. Therefore, the leakage current is so large that the polarization is hard to be measured mainly due to the low applied electric field. Furthermore, BFO has a G-type antiferromagnetic helical structure and thus limits the observation of ferromagnetism.

Alternatively, multiferroic composite, which is composed of ferromagnetic phase and ferroelectric phase, can produce ME effect through interfacial contact between the two phases. It is generally acknowledged that the ME effect of magnetoelectric composites is the result of magnetostrictive effect of the ferromagnetic phase and piezoelectric effect of the ferroelectric phase. When an external magnetic field is applied to the composites, a deformation of the ferromagnetic phase will be induced because of the magnetostrictive effect. As a consequence, a stress will transfer to the ferroelectric phase through the interface, and the electric properties of the ferroelectric phase can be varied due to the inverse piezoelectric effect. Conversely, when applying an electric field, the magnetization can be changed because of the counter magnetostriction effect of ferromagnetic materials. The advantage of composites is that the ferromagnetic and ferroelectric phases can play their individual roles, therefore the limitation of the Curie temperature in single phase multiferroics is absent. Compared with single-phase multiferroic materials, composite multiferroic materials have a variety of synthesis methods and various connective types, and thus they have strong magnetoelectric effects at room temperature, which is more convenient than single phase multiferroic materials.

It is not too difficult to imagine that the ME effect of magnetoelectric composites depends strongly on the intrinsic properties of the magnetic and ferroelectric phases such as the magnetostriction and piezoelectric coefficients as well as the conductivity. In addition, the connective style, molar ratio between two phases, and the interface also can determine the ME effect. Till now, many magnetoelectric systems have been investigated including $BaTiO_3/CoFe_2O_4$ [15], $BaTiO_3/Ni_{0.5}Zn_{0.5}Fe_2O_4$ [16], $Co_{0.6}Cu_{0.3}Zn_{0.1}Fe_2O_4/Ba_{0.9}Sr_{0.1}Zr_{0.1}Ti_{0.9}O_3$ [17], PZT/CFO [18], $Ni_{0.5}Zn_{0.5}Fe_2O_4/Pb_{0.8}Zr_{0.2}TiO_3$ [19], $SmFeO_3$/P(VDF-TrFE) [20], $Co_{0.8}Cu_{0.2}Fe_2O_4/Ba_{0.6}Sr_{0.4}TiO_3$ [21], $La_{0.7}Sr_{0.3}MnO_3/Pb(Mg_{1/3}Nb_{2/3})O_3$-$PbTiO_3$ [22], $GaFeO_3/Co_{0.5}Zn_{0.5}Fe_2O_4$ [23], $Bi_{0.5}Na_{0.5}TiO_3$-$Bi_{0.5}K_{0.5}TiO_3/Ni_{0.8}Zn_{0.2}Fe_2O_4$ [24] etc. Among them, $BaTiO_3$ based ferroelectric phase is one of the most studied materials in the magnetoelectric composites and ferrites are used as the conventional magnetic phases in the corresponding composites. It was reported that the incorporation of Zn^{2+} in $Co_{0.5}Zn_{0.5}Fe_2O_4$ ferromagnetic material makes the ferromagnetic material excellent in all aspects, with low coercivity, low dielectric loss, high electrical resistivity, high magnetic permeability, good chemical stability, large magnetic induction and magnetocrystalline anisotropy. It is a ferrite with excellent performance, whose magnetic spectrum characteristics are great, and it has a broad prospect at the low energy loss in the high frequency and ultra-high frequency state [25,26]. Therefore, this material is very suitable for high-density magnetic storage, such as magnetic recording materials or magneto-optical recording materials, as well as electromagnetic microwave absorption, magnetic fluid, drug targeting, magnetic resonance and airflow sensors [27]. In addition, it is well known that barium titanate has the characteristics of high dielectric constant, low dielectric loss and structural stability. The Curie temperature of $BaTiO_3$ can be changed by substitution of Ba^{2+} with Sr^{2+}, and $Ba_{1-x}Sr_xTiO_3$ (BST) not only has high dielectric constant, good dielectric non-linearity and low dielectric loss, but also has excellent piezoelectric properties, great pressure resistance and insulation properties [28–30].

Herein, $Co_{0.5}Zn_{0.5}Fe_2O_4$ (CZFO) is used as the magnetic phase while $Ba_{0.8}Sr_{0.2}TiO_3$ (BST) was selected as the ferroelectric phase. Co-precipitation method combined with sol-gel method was used to prepare ferromagnetic materials CZFO and ferroelectric materials BST, respectively. In this paper, the effects of molar ratio of CZFO to BST on the microstructure, dielectric, ferroelectric, magnetic and conductive properties of CZFO/BST composite ceramics were studied.

II. Experimental details

$Co_{0.5}Zn_{0.5}Fe_2O_4$ (CZFO) powder was prepared by co-precipitation method starting from $Co(NO_3)_2 \cdot 6H_2O$ (AR,98.0%), $Fe(NO_3)_3 \cdot 9H_2O$ (AR, 98.5%), $Zn(NO_3)_2 \cdot 6H_2O$ (AR, 98.0%), NaOH (AR, 96.0%). Appropriate amounts of raw materials were dissolved in distilled water at 80 °C, then they were mixed and stirred continuously, heated to 100 °C, and kept for 2 h. After cooling to room temperature naturally, the obtained product was ceaselessly washed with distilled water and then calcined at 700 °C (with heating rate of 5 °C/min) for 3 h in air to form CZFO powder. $Ba_{0.8}Sr_{0.2}TiO_3$ sol was prepared by sol-gel method starting from $Ba(CH_3COO)_2$ (AR, 99.9%), $Sr(CH_3COO)_2$

(AR, 98.0%), $Ti(OC_4H_9)_4$ (AR, 99.0%), CH_3COOH (AR, ≥99.5%), $CH_3C(=O)CH_2C(=O)CH_3$ (AR, ≥99.0%). Stoichiometric amounts of $Ba(CH_3COO)_2$ and $Sr(CH_3COO)_2$ were firstly weighed and then dissolved in CH_3COOH solution. After adding 2 drops of $C_5H_8O_2$ solution, it was heated at 60 °C in water bath and stirred for 10 min. Then the solution was added into appropriate amount of $Ti(OC_4H_9)_4$ solution, stirred for 20 min, finally the appropriate amount of $HO(CH_2CH_2O)_nH$ powder was added. When it was dissolved completely, stirred in a water bath at 80 °C for 2 h, aged for 2 days and the BST sol was obtained. CZFO/BST composite powders, with different molar ratios (1:3, 1:2, 1:1, 2:1 and 3:1), were prepared through adding CZFO magnetic powder to BST sol under constant stirring and heating until the sol became dry gel. Then the CZFO/BST mixed powders were mixed with appropriate amount of polyvinyl alcohol (PVA, 15 wt.%) as binder and uniaxially pressed into pellet with the diameter of 10 mm and thickness of 1 mm at 15 MPa for 10 min. The pellet was sintered at 1100 °C with the heating rate 5 °C/min for 3 h in air.

The phase of CZFO/BST ceramics was analysed by X-ray diffractometer (XRD, Rigaku D/max2400, 40 kV, 30 mA, CuKα, λ = 0.15406 nm) in the sweeping range of 2θ = 20–80° and scanning speed of 0.05 °/s. The surface morphology of the ceramics was observed using a scanning electron microscope (SEM, S-3700N, Hitachi, Japan). The CZFO/BST ceramics was polished and the silver paste was sintered at 800 °C for 30 min to make a silver electrode. Dielectric temperature characteristics of CZFO/PZT ceramics in the temperature range of 25 to 500 °C were tested using an LCR digital bridge (E4980A, Agilent, USA). The leakage current curves and ferroelectricity of the prepared CZFO/BST ceramics were tested in a LM mode and a PM mode using a ferroelectric analyser (TF2000E, aix-ACCT, Germany). The hysteresis loop of the CZFO/PZT ceramics was tested using a vibrating sample magnetometer (Quantum Design).

III. Results and discussion

3.1. Crystal structures

X-ray diffraction patterns of the CZFO/BST composite ceramics prepared at different ratios and of the corresponding single-phase ferroelectric (BST) and ferromagnetic (CZFO) samples are presented in Fig. 1. The patterns show that all the diffraction peaks of the composite ceramics correspond to the single-phase perovskite and ferrite structures with a small amount of $Ba_2Fe_2Ti_4O_{13}$ impurity phase. As can be seen from Fig. 1, all the diffraction peaks can be aligned in ceramics with the ratio of (3:1 2:1, 1:1, 1:2 and 1:3), and the diffraction peaks of the ceramics with the ratio of 1:2 are the highest. With the increase of CZFO content, the peak intensity at 35.6° is enhanced, but the peak intensity at 57° is weakened. It can also be seen that the peak intensity of the impurity $Ba_2Fe_2Ti_4O_{13}$ phase first increased and then weakened as the CZFO content increases. Due to the interfacial effect, Fe, Ba and Ti ions in the ferroelectric and ferromagnetic phases may migrate and diffuse at the interface to form $Ba_2Fe_2Ti_4O_{13}$ compound.

3.2. Surface morphology

Figure 2 shows the SEM images of the sample cross sections for different molar ratios. Before measuring the images, the samples were annealed at 1050 °C for 30 min. In these magnetoelectric composites, it may be speculated that two kinds of grain are ascribed to two different phases (CZFO and BST). The surface morphology of the ceramics is not flat, the large grains are about 2–3 μm, and the smallest grain size is ~0.5 μm. With the increase of BST content, the number of large crystal grains of the composite ceramics tends to decrease, indicating that the addition of a certain amount of BST is beneficial to the grain refinement to some extent.

In order to investigate the chemical composition of the composites, EDX maps related to the SEM images are presented in Figs. 3b and 3d. The content of each element was derived from the area marked in Figs. 3a and 3c. The obtained results proved that the larger grains are ascribed to CZFO phase.

Density of the composite ceramics decreases with the increase of BST content (Table 1). The growth of many small crystal grains does not contribute to the densification process enough. Thus, there are many pores and the growth directions of the crystal grains are inconsistent.

3.3. Dielectric properties

The relationship between the dielectric constant and dielectric loss of the CZFO/BST composite ceramics is shown in Fig. 4. The dielectric constant of all samples decreases with increasing frequency, as shown in Fig. 4a. Under high frequency conditions (at 1 MHz), the composite ceramics with the molar ratio of 1:2 has the largest dielectric constant (295), while the compos-

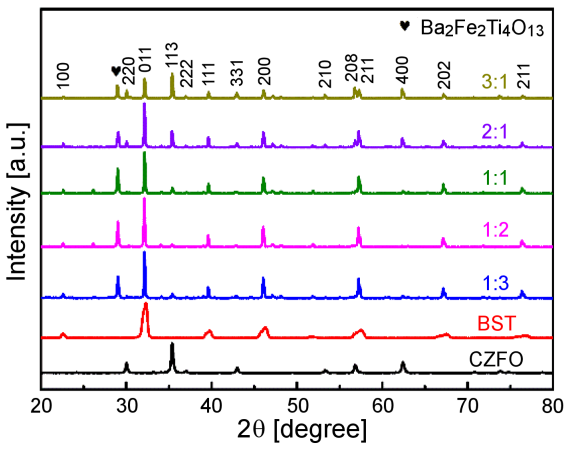

Figure 1. XRD patterns of CZFO, BST and CZFO/BST composite ceramics

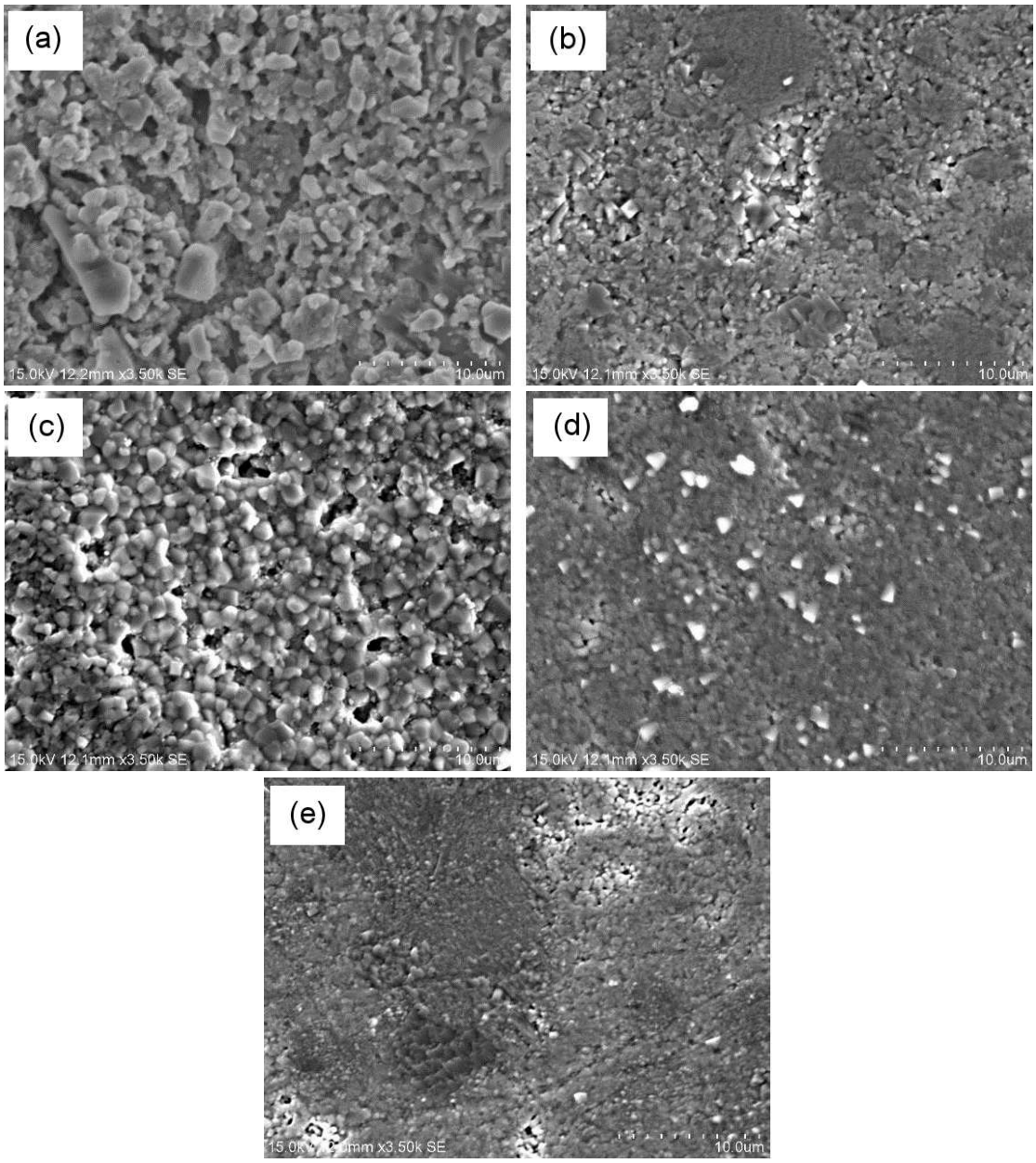

Figure 2. SEM images of CZFO/BST composites with different molar ratios: a) 3:1; b) 2:1, c) 1:1, d) 1:2 and e) 1:3

Table 1. Density of composite ceramics

Molar ratio	3:1	2:1	1:1	1:2	1:3
Actual density [g/cm^3]	4.82	4.80	4.94	4.63	4.50
Theoretical density [g/cm^3]	5.64	5.65	5.86	6.00	6.07
Density [%TD]	85.5	85.0	84.3	77.2	74.1

ite ceramics with molar ratio of 3:1 shows the minimum dielectric constant (32.8). With the increase of BST content (except for ratio of 1:3), the dielectric constant increases. This is because the dielectric properties of BST phase are better than that of CZFO phase, therefore dielectric behaviour is mainly provided by the ferroelectric phase (BST).

It can be concluded from Fig. 4b that with the increase of BST content, the dielectric loss of all the composite ceramics has a non-monotonic change. At high frequencies the dielectric loss is small and the composite ceramics with the molar ratio of 3:1 has the largest loss in almost all frequency ranges. It is worth mentioning that the smallest loss has the sample with the molar ratio of 2:1. Generally, the dielectric loss is contributed by three parts, including relaxation loss, conductive loss and resonance absorbing loss. Among them, resonance absorbing loss only occurs at very high frequency (at least 10^{15} Hz). Therefore, at the test frequency range (from 20 Hz to 2 MHz), relaxation loss and conductive

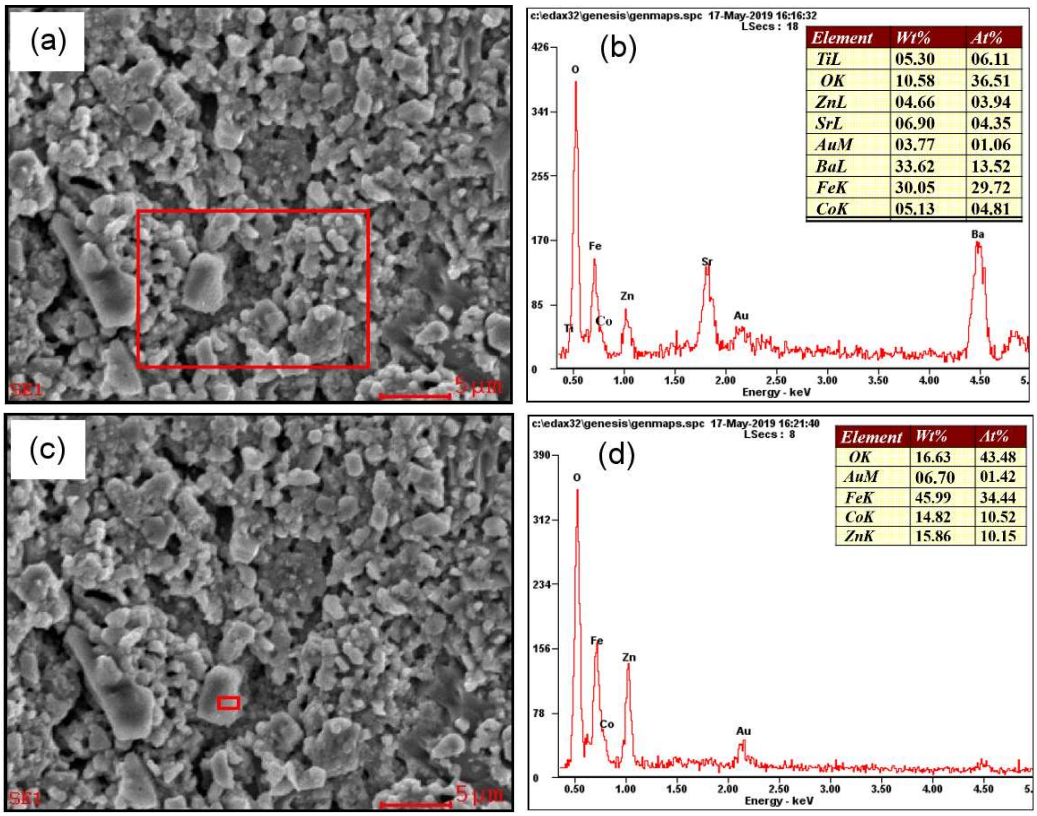

Figure 3. EDS and SEM images of CZFO/BST composites with two different molar ratios: 3:1 (a,b) and 2:1 (c,d)

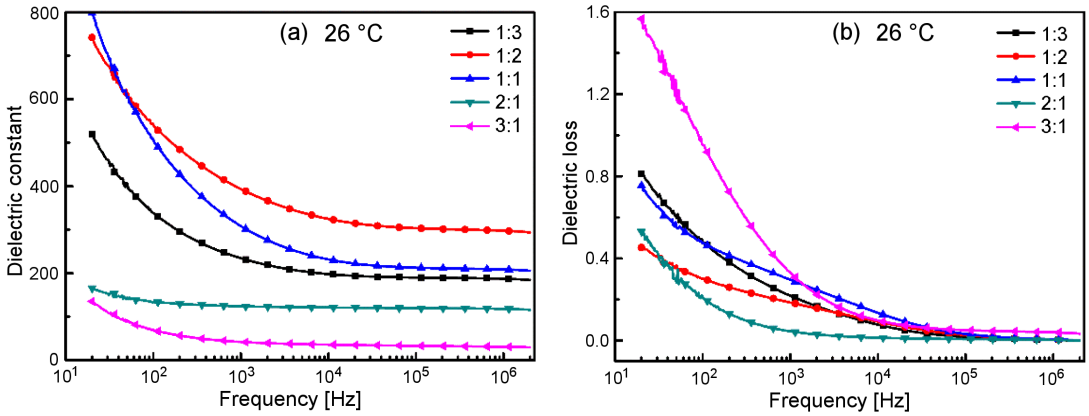

Figure 4. Frequency dependence of dielectric constant (a) and dielectric loss (b) of CZFO/BST composites with different molar ratios

loss are the main contributions to the dielectric loss. The relaxation loss includes space charge, interface, turning direction and ions relaxation polarization. However, the difference between these kinds of relaxation polarizations in different specimens is not distinct enough. The conductive loss is induced by the fact that these samples are not ideal insulators. In general, the conductivity of ferrite CZFO is larger than that of BST, therefore, the conductive loss of CZFO is also larger than that of BST. As a consequence, the conductive loss should increase with increasing the content of CZFO in the composites. Actually, other factors such as impurities, defects such as oxygen vacancies, pores, can affect the conductivity of the samples. Thus, the reason for the smallest loss of the sample 2:1 may be that the content of heterogeneous $Ba_2Fe_2Ti_4O_{13}$ in the sample 2:1 is the lowest, so that the contribution of conduction loss is reduced.

The dielectric loss of the CZFO/BST composite ceramics as a function of temperature is shown in Fig. 5. The characteristic loss peak can be observed. This peak moves towards the high temperature region, but the peak intensity increases slightly with the frequency. For example, when the frequency is 200 Hz, the peak of all the specimens is near 150 °C, while the peak position moves to about 400 °C when the frequency is 200 kHz. Obviously, this loss peak is generated by relaxation polarization. It should be pointed out that the fluctuation of the dielectric loss tends to be gentle for the sample with the

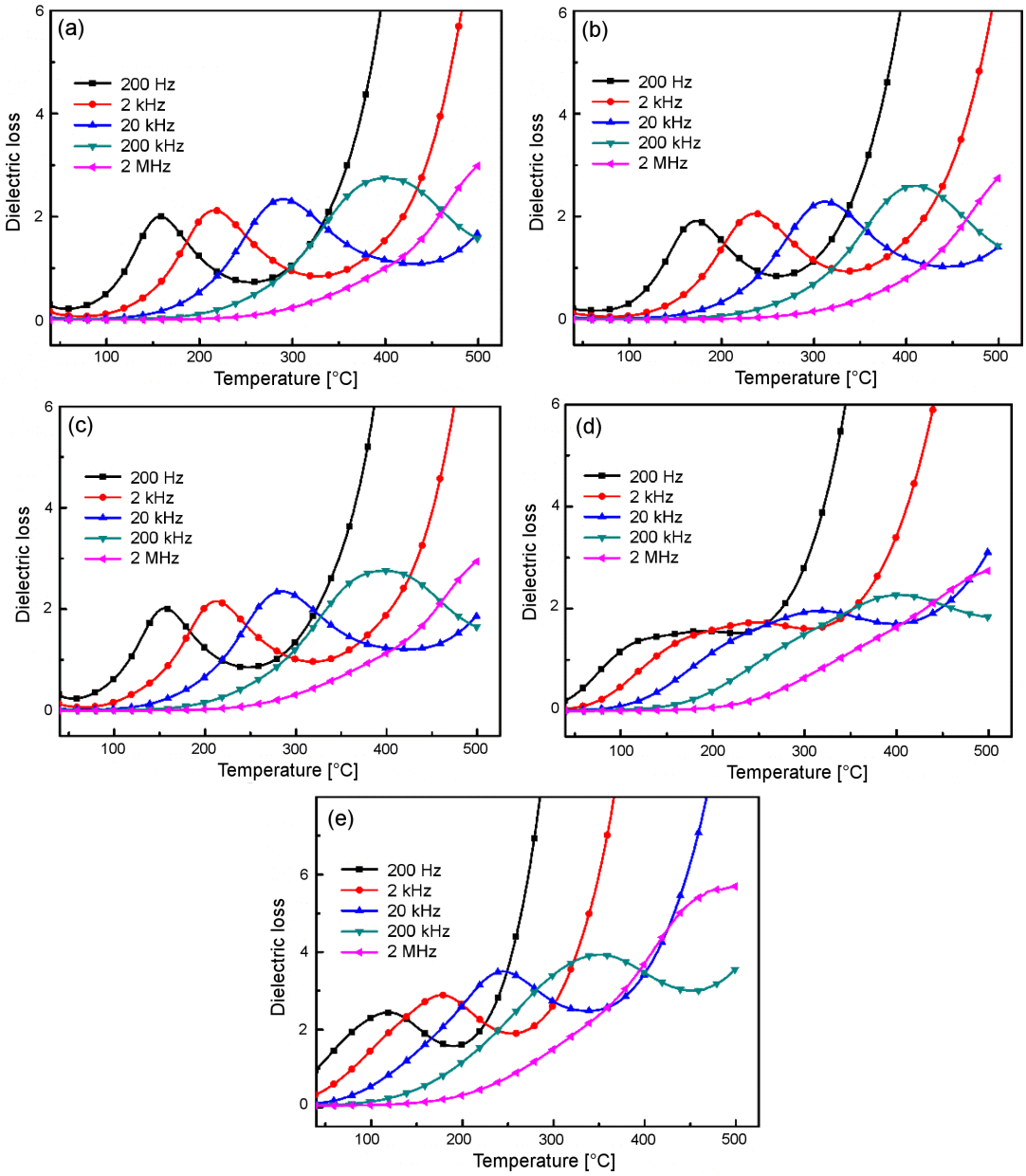

Figure 5. Temperature dependence of dielectric loss of the ceramics with different molar ratios: a) 1:3, b) 1:2, c) 1:1, d) 2:1 and e) 3:1

molar ratio of 2:1, and the peak has been broaden, as depicted in Fig. 5d. The dielectric loss is mainly caused by relaxation polarization and leakage conductance. When the frequency of the external electric field increases by a certain value, the relaxation polarization cannot keep up with the change of the external electric field, so the dielectric loss is reduced [21,31]. The curve fluctuation of the sample with the molar ratio of 2:1 is not obvious, which may be due to the less relaxation polarization induced by impurities in the sample.

Figure 6 presents the temperature dependence of dielectric constant of the CZFO/BST composite ceramics. It can be seen that with the frequency increase, the dielectric constant (ε_r) decreases. In the low temperature region, ε_r increases slowly with increasing temperature, as the temperature further increases (above 250 °C), ε_r increases sharply. This may be ascribed to two reasons. On one hand, a high temperature can increase the electronic transition between Fe^{2+} and Fe^{3+} in the ferrite, resulting in a sharp increase of ε_r and enhanced ion polarization [32,33]. On the other hand, the increased dielectric constant is due to the space charge polarization effect at the interface of CZFO and BST phase [34,35]. In addition, more free electrons can be generated at higher temperature, and thus larger polarization is induced. When the frequency is high, the dielectric constant is determined only by the displacement polarization, so the dielectric loss induced by polarization tends to be minimal but the leakage current increases promptly because more electrons can be motivated from the valance band and then jump into the conductive band, inducing the increase of carrier density.

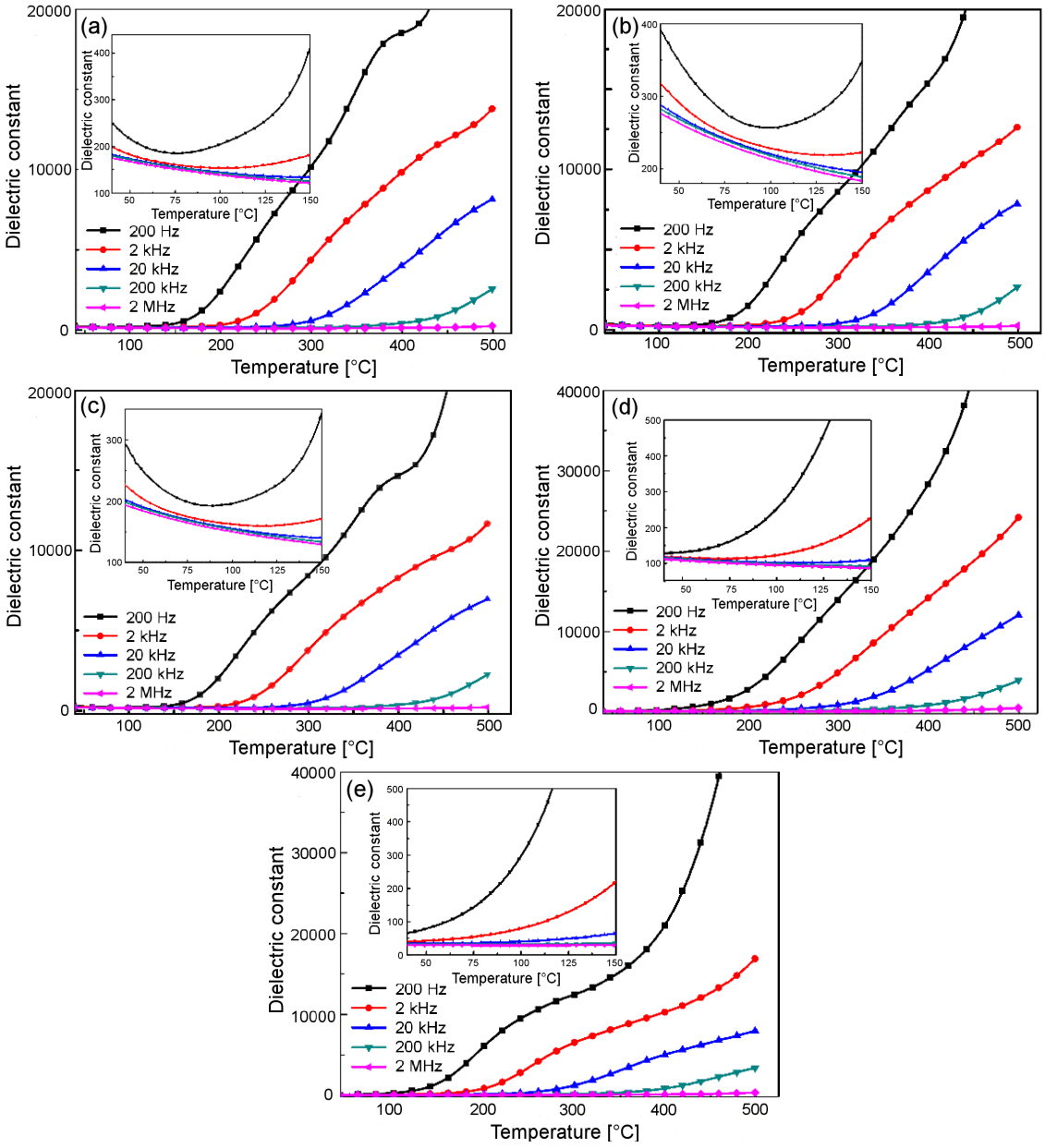

Figure 6. Dielectric constant as a function of temperature for the ceramics with different molar ratios: a) 1:3, b) 1:2, c) 1:1, d) 2:1 and e) 3:1

To comparatively research the different dielectric properties among these samples, dielectric constant and dielectric loss as a function of temperature measured at a frequency of 20 kHz are shown in Fig. 7. The dielectric constant does not change much at low temperatures. When the temperature rises to ~250 °C, the dielectric constant begins to increase obviously. The dielectric constant increases sharply at about 330 °C. It was mentioned above that this abrupt increase of dielectric constant at about 330 °C is a result of the abundant increase of carriers which were motivated from the valance band at high temperature. With the increase of BST content, the dielectric constant increases at first and then decreases at low temperature (approximately <180 °C), and it has an opposite trend at high temperatures. That is related to the interfacial interaction between the ferroelectric phase and the ferromagnetic phase. In fact, the grain size, grain boundary and density can affect the dielectric constant.

As shown in Fig. 7b, the dielectric loss increases at first and then decreases and starts to increase again with increasing temperature. This peak of loss is related to the relaxation polarization. When the temperature rises, the relaxation polarization increases, the ion motion is more intense, the relaxation time decreases, so the dielectric loss increases. When the temperature is higher than a certain degree, the directional migration of the ions is hindered by the thermal motion, and the polarization is weakened. The peak position variation with molar ratio can be noticed in the plots of dielectric loss in Fig. 7b. The peak of the sample with the molar ratio of 1:2 corresponds to the highest temperature.

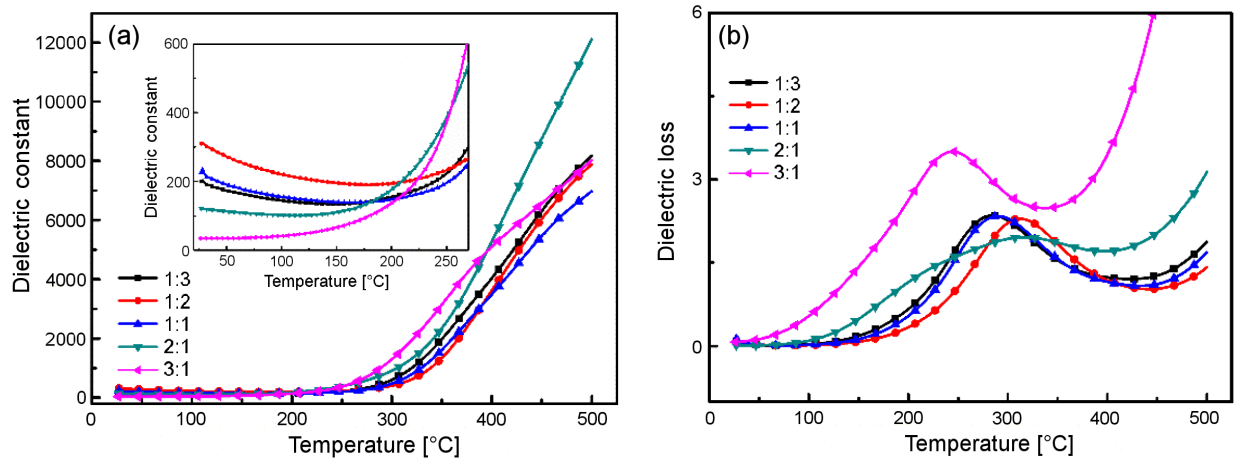

Figure 7. Dielectric constant and dielectric loss as a function of temperature measured at 20 kHz

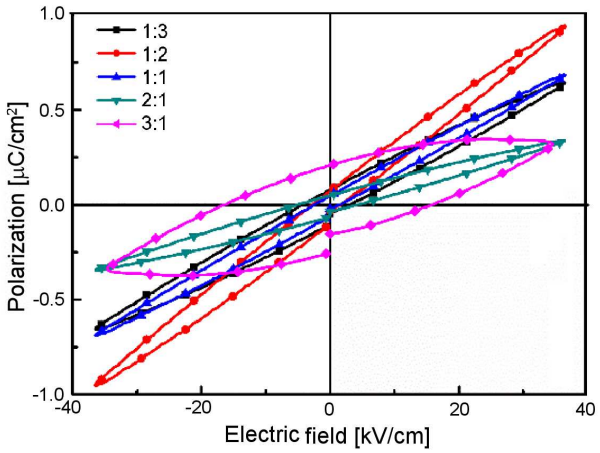

Figure 8. Hysteresis loops of CZFO/BST composite ceramics with different molar ratios

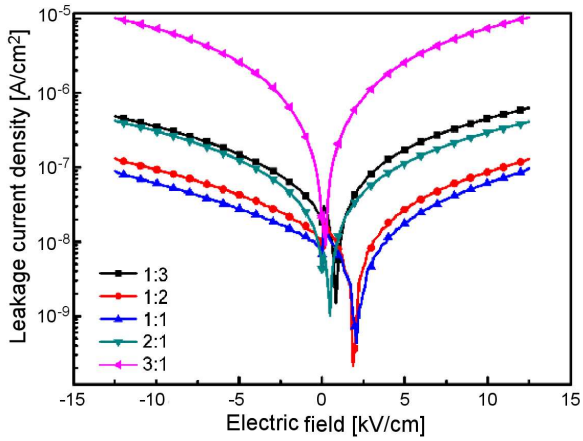

Figure 9. Leakage current as a function of applied field of CZFO/BST composite ceramics with different molar ratios

3.4. Ferroelectric properties

Figure 8 shows room temperature hysteresis loops of the CZFO/BST composite ceramics with different ratios with the maximal electric field of 36 kV/cm and frequency of 1 kHz. The remnant polarization (P_r) and the coercive field (E_c) decrease at first and then increase with the increase of CZFO content. The ferroelectric properties are mainly contributed by the BST phase. The value of P_r is 0.189 μC/cm^2 for the sample with the molar ratio of 1:3 and increases to 0.465 μC/cm^2 for the sample with the molar ratio of 3:1. This trend dose not characterize the ferroelectric properties of the composites. With the increase of CZFO content, the space charge effect has a bigger contribution to composites [36]. Besides, the area of the hysteresis loop of the sample with the molar ratio of 3:1 is very large. The reason is that the resistivity of CZFO is smaller than that of BST, therefore, the addition of CZFO increases the electrical conductivity of the ceramics, making the ferroelectric performance worse [24]. These results have proven that the addition of CZFO to BST has a great influence on the ferroelectric properties of BST.

In order to elucidate whether the leakage currents in these samples are varied with molar ratio, the current was measured as a function of applied field. Figure 9 illustrates room temperature leakage current versus field of the prepared CZFO/BST composite ceramics with different ratios. The composite ceramics with the molar ratio of 3:1 has the largest leakage current (1.06×10^{-5} A/cm^2 at 1.5 kV/cm), and the composite ceramics with the molar ratio of 1:1 has the minimum leakage current (8.10×10^{-8} A/cm^2). In general, the leakage current is mostly induced by CZFO component because as a typical dielectric material, the electrical resistivity of BST is much larger than that of CZFO. Therefore, this result of leakage current indicates that in addition to the intrinsic conductive properties, the content of CZFO has a large influence on the leakage current of the composite ceramics. When the CZFO content is high, the ceramics will have more defects, which will reduce the density of the ceramics and it is consistent with the SEM results. Besides, one can note that the composite ceramics with other molar ratios (1:3, 1:2 and 1:1) have a shift of the *x*-axis origin in the leakage current curves, and the composite ceramics with molar ratio of 1:3 has the most offset. This phenomenon is usually attributed to the formation of internal field between the sample and the top and bottom electrodes in the preparation process [37].

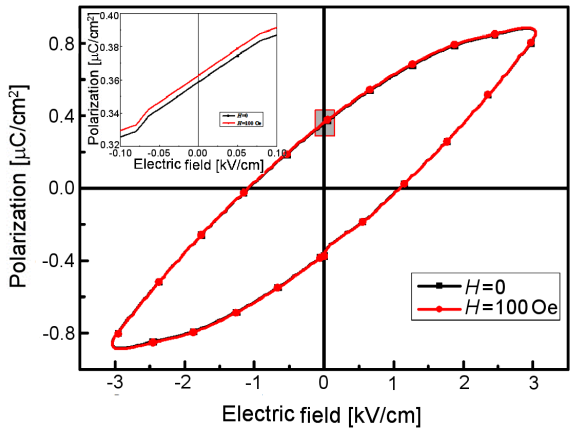

Figure 10. Hysteresis loops of CZFO/BST composite ceramics with or without applying magnetic field

The magnetoelectric coupling effect is one of the most important properties of multiferroic material. Due to the technical limitations, we can only measure the ferroelectric hysteresis loop under the action of external magnetic field. Figure 10 shows the hysteresis loops of the composite ceramics with the molar ratio of 1:3 under the influence of the applied magnetic field at frequency of 1 kHz. It can be seen from Fig. 10 that the presence or absence of the magnetic field (100 Oe) has little effect on the ferroelectric properties of the material. This indicates that the sample shows weak magnetoelectric coupling effect.

3.5. Magnetic properties

Magnetic hysteresis loops of the CZFO/BST composite ceramics with different molar ratios are shown in Fig. 11, and the corresponding magnetic parameters are listed in Table 2. It can be seen that the values of remnant magnetization (M_r) and saturation magnetization (M_s) of the sample with the molar ratio of 3:1 are about 0.46 emu/g and 50.3 emu/g, respectively. With the increase of CZFO content, both M_s and M_r values decrease at first and then increase apparently. It is interesting that the magnetization of the sample with the molar ratio 1:3 (the content of BST is the largest) is the third largest. Normally, the magnetization of the composites is mainly contributed by the magnetic phase. Therefore, the magnetization should be proportional to the content of CZFO in the composites. The grain size, grain shape and some undetected impurities can influence magnetic properties to some extent and thus can affect the total magnetic behaviours in these composites. However, the abnormally enhanced magnetization of the sample (molar ratio is 1:3) can be deemed to be the result of strong interface interaction between the two phases [38], and this anomalous magnetic behaviour has also been observed in other magnetoelectric composites [17,19]. This stronger interaction may be due to the high content of BST phase. The effective specific interface area between the two phases may be increased because more magnetic grains can be surrounded by the BST phase. Therefore, the distribution of magnetic ions and their spin orientation are changed, thus the magnetic properties of the ceramic composites are affected.

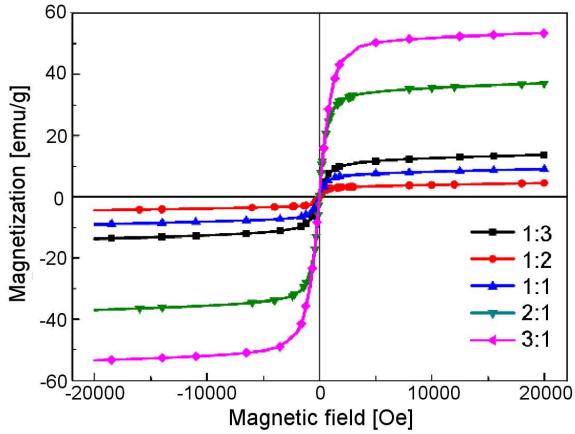

Figure 11. Magnetization versus magnetic field of CZFO/BST composite ceramics with different molar ratios

Table 2. Saturated magnetization (M_s) and remnant magnetization (M_r) of CZFO/BST ceramics with different ratios

Molar ratio	3:1	2:1	1:1	1:2	1:3
M_s [emu/g]	11.3	3.36	6.62	33.4	50.3
M_r [emu/g]	0.27	0.03	0.07	0.12	0.46

IV. Conclusions

$Co_{0.5}Zn_{0.5}Fe_2O_4/Ba_{0.8}Sr_{0.2}TiO_3$ (CZFO/BST) composite ceramics have been successfully synthesized by combining co-precipitation with sol-gel method. XRD analysis revealed the presence of a heterogeneous $Ba_2Fe_2Ti_4O_{13}$ phase in the sample, which was related to chemical reaction at the interface. The composite ceramics with the molar ratio of 1:2 can reach a dielectric constant of 295 at high frequency (1 MHz), and the composite ceramics with a molar ratio of 3:1 has the largest (1.59) loss at low frequency. The remnant polarization of the composite with a molar ratio of 1:2 is the largest (0.42 μC/cm^2). The composite ceramics with molar ratios of 1:3, 1:2 and 1:1 have unsymmetrical *J-E* curves along the axes as a result of the interface barrier. The remnant magnetization of the composite ceramics with the molar ratio of 3:1 is the largest (0.46 emu/g), and the saturation magnetization is also the largest (50.3 emu/g) because of the larger content of the magnetic phase CZFO. The magnetization of the sample with the lowest content of CZFO shows better magnetic properties than other samples except of the samples with the molar ratio 2:1 and 3:1. This anomalous enhancement of magnetic properties can be attributed to the strongest interface interaction between CZFO and BST grains. The reason is that larger interface areas between the two phases can be formed when the content of CZFO is at the minimum. Our results may provide some useful information for enhancing multiferroic properties by tuning interface effect.

Acknowledgement: The present work has been supported by the Chongqing Research Program of Basic Research and Frontier Technology (CSTC2018jcyjAX0416, CSTC2019jcyj-msxmX0071), the Science and Technology Research Program of Chongqing Municipal Education Commission (KJZD-M201901501), the Scientific and Technological Research Young Program of Chongqing Municipal Education Commission (KJQN201801509, KJQN20190150), the Program for Creative Research Groups in University of Chongqing (Grant No. CXQT19031), the Innovation Program for Chongqing's Overseas Returnees (cx2019159), the Excellent Talent Project in University of Chongqing (Grant No. 2017-35), the Science and Technology Innovation Project of Social Undertakings and Peoples Livelihood Guarantee of Chongqing (cstc2017shmsA90015), the Program for Innovation Teams in University of Chongqing, China (CXTDX201601032), the Leading Talents of Scientific and Technological Innovation in Chongqing (CSTCCXLJRC201919), the Program for Technical and Scientific Innovation Led by Academician of Chongqing, the Latter Foundation Project of Chongqing University of Science & Technology (CKHQZZ2008002), and the Scientific & Technological Achievements Foundation Project of Chongqing University of Science & Technology (CKKJCG2016328), the Postgraduate technology innovation project of Chongqing University of Science & Technology (YKJCX1820214) and the student innovating projects of science of Chongqing (YKJCX1820205).

References

1. S. Zhao, Z. Zhou, B. Peng, M. Zhu, M. Feng, Q. Yang, Y. Yan, W. Ren, Z. Ye, Y. Liu, M. Liu, "Quantitative determination on ionic-liquid-gating control of interfacial magnetism", *Adv. Mater.*, **29** (2017) 1606478.
2. M. Liu, O. Obi, J. Lou, Y. Chen, Z. Cai, S. Stoute, M. Espanol, M. Lew, X. Situ, K.S. Ziemer, V.G. Harris, N.X. Sun, "Giant electric field tuning of magnetic properties in multiferroic ferrite/ferroelectric heterostructures", *Adv. Funct. Mater.*, **19** (2009), 1826–1831.
3. R.L. Gao, H.W. Yang, J.R. Sun, Y.G. Zhao, B.G. Shen. "Oxygen vacancies induced switchable and nonswitchable photovoltaic effects in $Ag/Bi_{0.9}La_{0.1}FeO_3/La_{0.7}Sr_{0.3}MnO_3$ sandwiched capacitors", *Appl. Phys. Lett.*, **104** (2014) 031906.
4. D.R. Patil, B.K. Chougule, "Structural, electrical and magnetic properties of xNiFe$_2$O$_4$ + (1-x)Ba$_{0.8}$Sr$_{0.2}$TiO$_3$ ME composites", *J. Alloys Compds.*, **458** (2008) 335–339.
5. R.L. Gao, L. Bai, Z.Y. Xu, Q. M. Zhang, Z.H. Wang, W. Cai, G. Chen, X.L. Deng, C.L. Fu, "Electric-field induced magnetization rotation in magnetoelectric multiferroic fluids", *Adv. Electr. Mater.*, **4** (2018) 1800030.
6. J.A. Paulsen, A.P. Ring, C.C.H. Lo, J.E. Snyder, D.C. Jiles, "Manganese-substituted cobalt ferrite magnetostrictive materials for magnetic stress sensor applications", *J. Appl. Phys.*, **97** (2005) 044502.
7. R.L. Gao, H.W. Yang, C.L. Fu, W. Cai, G. Chen, X.L. Deng, J.R. Sun, Y.G. Zhao, B.G. Shen, "Tunable photovoltaic effects induced by different cooling oxygen pressure in $Bi_{0.9}La_{0.1}FeO_3$ thin films", *J. Alloys Compds.*, **624** (2015) 1–8.
8. W. Eerenstein, N.D. Mathur, J.F. Scott, "Multiferroic and magnetoelectric materials", *Nature*, **442** (2006) 759–765.
9. Z.X. Li, Z.H. Wang, R.L. Gao, W. Cai, G. Chen, X.L. Deng, C.L. Fu, "Dielectric, ferroelectric and magnetic properties of $Bi_{0.78}La_{0.08}Sm_{0.14}Fe_{0.85}Ti_{0.15}O_3$ ceramics prepared at different sintering conditions", *Process. Appl. Ceram.*, **12** (2018) 394–402.
10. W. Prellier, M.P. Singh, P. Murugavel, "The single-phase multiferroic oxides: From bulk to thin film", *J. Phys. Condens. Mat.*, **17** (2005) R803–R832.
11. R.L. Gao, C.L. Fu, W. Cai, G. Chen, X.L. Deng, H.R. Zhang, J.R. Sun, B.G. Shen, "Electric control of the hall effect in $Pt/Bi_{0.9}La_{0.1}FeO_3$ bilayers", *Sci. Reports*, **6** (2016) 20330.
12. G.S. Arya, R.K. Kotnala, N.S. Negi, "Enhanced magnetic and magnetoelectric properties of In and Co codoped $BiFeO_3$ nanoparticles at room temperature", *J. Nanopart. Res.*, **16** (2014) 2155.
13. S.V. Vijayasundaram, G. Suresh, R.A. Mondal, R. Kanagadurai, "Composition-driven enhanced magnetic properties and magnetoelectric coupling in Gd substituted $BiFeO_3$ nanoparticles", *J. Magn. Magn. Mater.*, **418** (2016) 30–36.
14. J.M. Caicedo, J.A. Zapata, M.E. Gómez, P. Prieto, "Magnetoelectric coefficient in $BiFeO_3$ compounds", *J. Appl. Phys.*, **103** (2008) 07E306.
15. R.L. Gao, Q.M. Zhang, Z.Y. Xu, Z.H. Wang, W. Cai, G. Chen, X.L. Deng, X.L Cao, X. D. Luo, C.L. Fu, "Strong magnetoelectric coupling effect in $BaTiO_3$@$CoFe_2O_4$ magnetoelectric multiferroic fluids", *Nanoscale*, **10** (2018) 11750–11759.
16. L.P. Curecheriu, M.T. Buscaglia, V. Buscaglia, L. Mitoseriu, P. Postolache, A. Ianculescu, P. Nanni, "Functional properties of $BaTiO_3$-$Ni_{0.5}Zn_{0.5}Fe_2O_4$ magnetoelectric ceramics prepared from powders with core-shell structure", *J. Appl. Phys.*, **107** (2010) 104106.
17. R.L. Gao, Q.M. Zhang, Z.Y. Xu, Z.H. Wang, G. Chen, X.L. Deng, C.L. Fu, W. Cai, "A comparative study on the structural, dielectric and multiferroic properties of $Co_{0.6}Cu_{0.3}Zn_{0.1}Fe_2O_4/Ba_{0.9}Sr_{0.1}Zr_{0.1}Ti_{0.9}O_3$ composite ceramics", *Composites Part B*, **166** (2019) 204–212.
18. N. Ortega, A. Kumar, R.S. Katiyar, C. Rinaldi, "Dynamic magneto-electric multiferroics PZT/CFO multilayered nanostructure", *J. Mater. Sci.*, **44** (2009) 5127–5142.
19. R.C. Xu, Z.H. Wang, R.L. Gao, S.L. Zhang, Q.W. Zhang, Z.D. Li, C. Y. Li, G. Chen, X.L. Deng, W. Cai, C.L. Fu, "Effect of molar ratio on the microstructure, dielectric and multiferroic properties of $Ni_{0.5}Zn_{0.5}Fe_2O_4$-$Pb_{0.8}Zr_{0.2}TiO_3$ nanocomposite", *J. Mater. Sci.: Mater. Electron.*, **29** (2018) 16226–16237.
20. A. Ahlawat, S. Satapathy, M.M. Shirolkar, J.N. Li, A.A. Khan, P. Deshmukh, H.Q. Wang, R.J. Choudhary, A.K. Karnal, "Tunable magnetoelectric nonvolatile memory devices based on $SmFeO_3$/P(VDF-TrFE) nanocomposite films", *ACS Appl. Nano Mater.*, **1** [7] (2018) 3196–3203.
21. R.C. Xu, S.L. Zhang, F.Q. Wang, Q.W. Zhang, Z.D. Li, Z.H. Wang, R.L. Gao, C.L. Fu, "The study of microstructure, dielectric and multiferroic properties of (1-x) $Co_{0.8}Cu_{0.2}Fe_2O_4$-xBa$_{0.6}$Sr$_{0.4}$TiO$_3$ composites", *J. Electron. Mater.*, **48** (2019) 386–400.
22. H. Xu, M. Feng, M. Liu, X.D. Sun, L. Wang,

L.Y. Jiang, X. Zhao, C.W. Nan, A.P. Wang, H.B. Li, "Strain-mediated converse magnetoelectric coupling in $La_{0.7}Sr_{0.3}MnO_3$/$Pb(Mg_{1/3}Nb_{2/3})O_3$-$PbTiO_3$ multiferroic heterostructures", *Cryst. Growth Des.*, **18** [10] (2018) 5934–5939.

23. A. Ghani, S. Yang, S.S. Rajput, S. Ahmed, A. Murtaza, C. Zhou, Y. Zhang, X.P. Song, X.B. Ren, "Enhanced multiferroic properties of lead-free (1-x)$GaFeO_3$-(x)$Co_{0.5}Zn_{0.5}Fe_2O_4$ composites", *J. Appl. Phys.*, **124** (2018) 154101.
24. S. Liu, L.W. Deng, S.Q. Yan, H. Luo, L.L. Yao, L.H. He, Y.H. Li, M.Z. Wu, S.X. Huang, "Magnetoelectric properties of lead-free (80 $Bi_{0.5}Na_{0.5}TiO_3$-20 $Bi_{0.5}K_{0.5}TiO_3$)-$Ni_{0.8}Zn_{0.2}Fe_2O_4$ particulate composites prepared by in situ sol-gel", *J. Appl. Phys.*, **122** (2017) 034103.
25. R.T. Ma, H.T. Zhao, G. Zhang, "Preparation, characterization and microwave absorption properties of polyaniline/$Co_{0.5}Zn_{0.5}Fe_2O_4$ nanocomposite", *Mater. Res. Bull.*, **45** (2010) 1064–1068.
26. R. Arulmurugan, G. Vaidyanathan, S. Sendhilnathan, B. Jeyadevan, "Preparation and properties of temperature-sensitive magnetic fluid having $Co_{0.5}Zn_{0.5}Fe_2O_4$ and $Mn_{0.5}Zn_{0.5}Fe_2O_4$ nanoparticles", *Physica B*, **368** (2005) 223–230.
27. D. Varshney, K. Verma, A. Kumar, "Substitutional effect on structural and magnetic properties of $A_xCo_{1-x}Fe_2O_4$ (A = Zn, Mg and x = 0.0, 0.5) ferrites", *J. Mol. Structure*, **1006** (2011) 447–452.
28. C.R.K. Mohan, P.K. Bajpai, "Effect of sintering optimization on the electrical properties of bulk $Ba_xSr_{1-x}TiO_3$ ceramics", *Physica B - Condens. Mat.*, **403** (2008) 2173–2188.
29. C. Shen, Q. Liu, Q. F. Liu, "Photoluminescence properties of Er^{3+} doped $Ba_{0.5}Sr_{0.5}TiO_3$ prepared by sol-gel synthesis", *Mater. Sci. Eng.*, **111** (2004) 31–35.
30. W. Cai, C.L. Fu, Z. Lin, X. Deng, "Vanadium doping effects on microstructure and dielectric properties of barium titanate ceramics", *Ceram. Int.*, **37** (2011) 3643–3650.
31. R. Sharma, P. Pahuja, R.P. Tandonn, "Structural, dielectric, ferromagnetic, ferroelectric and ac conductivity studies of the $BaTiO_3$-$CoFe_{1.8}Zn_{0.2}O_4$ multiferroic particulate composites", *Ceram. Int.*, **40** (2014) 9027–9036.
32. L.P. Curecheriu, M.T. Buscaglia, V. Buscaglia, L. Mitoseriu, P. Postolache, A. Ianculescu, P. Nanni, "Functional properties of $BaTiO_3$-$Ni_{0.5}Zn_{0.5}Fe_2O_4$ magnetoelectric ceramics prepared from powders with core-shell structure", *J. Appl. Phys.*, **107** (2010) 104106.
33. R.F. Ziolo, "Synthesis and characterization of novel $CoFe_2O_4$-$BaTiO_3$ multiferroic core-shell-type nanostructures", *Acta Mater.*, **58** (2010) 764–769.
34. Z. Yu, C. Ang, "Maxwell-Wagner polarization in ceramic composites $BaTiO_3$-$(Ni_{0.3}Zn_{0.7})Fe_{2.1}O_4$", *J. Appl. Phys.*, **91** (2002) 794–797.
35. Y.J. Li, X.M. Chen, R.Z. Hou, Y.H. Tang, "Maxwell-Wagner characterization of dielectric relaxation in $Ni_{0.8}Zn_{0.2}Fe_2O_4$/$Sr_{0.5}Ba_{0.5}Nb_2O_6$ composite", *Solid State Commun.*, **137** (2006) 120–125.
36. R.Y. Zheng, J. Wang, S. Ramakrishna, "Electrical and magnetic properties of multiferroic $BiFeO_3$/$CoFe_2O_4$ heterostructure", *J. Appl. Phys.*, **104** (2008) 034106.
37. R.L. Gao, H.W. Yang,Y.S. Chen, J.R. Sun, Y.G. Zhao, B.G. Shen, "The study of open circuit voltage in Ag/$Bi_{0.9}La_{0.1}FeO_3$/$La_{0.7}Sr_{0.3}MnO_3$ heterojunction structure", *Physica B*, **432** (2014) 111–115.
38. R.L. Gao, Z.H. Wang, G. Chen, X.L. Deng, W. Cai, C.L. Fu, "Influence of core size on the multiferroic properties of $CoFe_2O_4$@$BaTiO_3$ core shell structured composites", *Ceram. Int.*, **44** (2018) S84–S87.